

Design and Performance of the Voltage Control Loop in Induction Heating Systems with L-LC Resonant Inverters

Mihaela Popescu* , Alexandru Bitoleanu* , Eugen Subțirelu*

* University of Craiova/Faculty of Electrical Engineering, Craiova, Romania, mpopescu@em.ucv.ro

* University of Craiova/Faculty of Electrical Engineering, Craiova, Romania, alex.bitoleanu@em.ucv.ro

* University of Craiova/Faculty of Electrical Engineering, Craiova, Romania, esubtirelu@em.ucv.ro

Abstract - In the induction heating systems¹ with voltage source inverter and resonant L-LC load, different ways to control the power transferred to the heated piece are possible. This paper takes into consideration separate control loops for the inverter frequency and the power flow and the focus is on the solution to regulate the inductor current through the inverter input voltage. A transfer functions based approach is adopted in the design of the control system. The types of controllers considered for the inverter input voltage control are proportional integral derivative and then proportional integral. The controllers tuning is achieved by using the Modulus Optimum criterion in Kessler variant. It is pointed out that the controller's parameters in both variants do not depend on the inverter load. The performances of the control system for both voltage controllers were tested and validated by simulation under the Matlab-Simulink environment by using real parameters of induction coils and heated pipes from a leading Romanian manufacturer. The results prove the very good behavior of the designed control loop with proportional integral derivative controller when both step and ramp input signal are applied. On the other hand, the performances obtained with a proportional integral controller are significantly weaker.

Keywords - induction heating, Modulus Optimum criterion, resonant inverter, PID controller, power control

I. INTRODUCTION

Different types of systems with load commutated inverters were used in induction heating applications. Most of them are based on single-phase current source inverters with parallel resonant load or voltage source inverters with series resonant load [1]-[7]. It was shown that the converter utilization is better in the case of the voltage source resonant inverters, especially in the high frequency area [1].

Although the traditional resonant circuit of the voltage source inverter is formed by the heating coil in series with a compensation capacitor, the researchers' studies have shown that a three element (L-LC) resonant load leads to a smaller current through the transformer secondary and an increased short-circuit immunity due to the inductive behavior of the load [2]-[5].

Different control strategies have been adapted for the resonant inverters in induction heating applications, such

as pulse amplitude modulation (PAM), pulse-frequency modulation (PFM), phase shift and pulse density modulation (PDM) [6], [7]. In [7], the L-LC resonant tank is designed with a matching transformer between the series inductor and the LC resonant circuit and the output power is controlled by the asymmetrical voltage cancellation technique.

In this paper, the attention is directed to the control of power transferred to the heated piece through the output inverter voltage, which means the control of the average voltage provided by the rectifier. Starting from the block diagram based on transfer functions, the Modulus Optimum (MO) criterion is successfully applied in tuning the voltage control loop.

II. STRUCTURE OF THE CONTROL SYSTEM

In the adopted induction heating system shown in Fig. 1, the resonant DC-link converter consists of a fully controlled three-phase bridge rectifier, a voltage DC-link circuit, an IGBTs-based single-phase full-bridge voltage source inverter, and a parallel resonant LC circuit coupled at the inverter output via a matching inductor [8].

To significantly reduce the inverter switching losses, the zero-current switching is under consideration. Therefore, the inverter operating frequency, which is controlled by an auto-adaptive loop, must be slightly higher than the resonant frequency of the equivalent circuit consisting of the induction coil-heated piece in parallel with the resonant capacitor.

The control of the heating inductor current can be achieved by controlling either the inverter output current [9], or the square-wave inverter voltage, respectively the average value of the voltage given by the rectifier to the inverter input.

If the frequency control loop is fast enough, the control of the current through inductor and the control of the inverter input voltage are practically equivalent.

III. TRANSFER FUNCTIONS BLOCK DIAGRAM

The forward path in the block diagram shown in Fig. 2 consists of transfer functions associated to the voltage controller $-G_{Ri}(s)$, three-phase rectifier $-G_R(s)$ and voltage DC-link $G_{DC}(s)$.

In the feedback path, the voltage transducer is assumed as an element of proportional type.

¹ This work is the result of research activity within Grant 352/21.11.2011, POSCCE-A2-O2.1.1-2011-2.

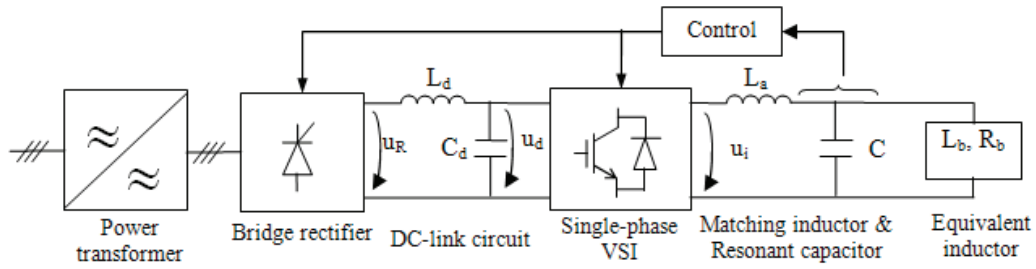


Fig. 1. Basic block diagram of the induction heating system.

The specific constants are [9]:

K_R – the proportional constant of the rectifier given by the rms secondary voltage of the power transformer;

T_μ – the rectifier integral time constant which corresponds to the average dead-time associated to the firing circuit;

$T_{ed} = R_d \cdot C_d$ and $T_{emd} = L_d / R_d$ – the electric and electromagnetic time constants of the DC-link circuit;

K_{Tu} – the proportional constant of the voltage transducer.

Thus, the transfer function of the fixed part of the unity feedback system is expressed as:

$$G_F(s) = \frac{K_R}{1 + sT_\mu} \cdot \frac{1}{1 + T_{ed}s + T_{emd}T_{ed}s^2} \cdot K_{Tu} \quad (1)$$

IV. VOLTAGE CONTROLLER DESIGN

A Proportional-Integral-Derivative (PID) controller and then a Proportional-Integral (PI) controller are to be designed in order to be used in the inverter input voltage control loop.

A. PID controller design

A PID controller can be adopted for the voltage controller in order to remove the dominant time constants (T_{ed} and T_{emd}). The associated proportional constant (K_p) and integral and derivative time constants (T_i and T_d) involved the transfer function expression,

$$G_{Ru}(s) = \frac{1 + K_p T_i s + T_i T_d s^2}{T_i s} \quad (2)$$

are to be determined.

The design of the voltage controller follows the principle of the Modulus Optimum criterion in Kessler variant, which is dedicated to the rapid systems [10], [11].

First, the open-loop unity feedback transfer function is expressed as:

$$G_{du}(s) = \frac{K_R \cdot K_{Tu} \cdot (1 + K_p T_i s + T_i T_d s^2)}{(1 + sT_\mu) \cdot s T_i \cdot (1 + T_{ed}s + T_{emd}T_{ed}s^2)} \quad (3)$$

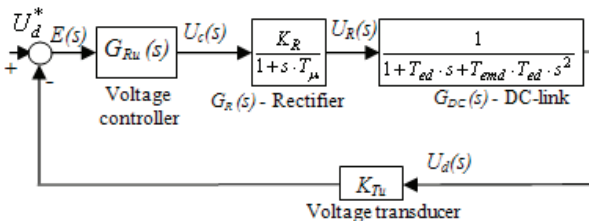


Fig. 2. Transfer functions based block diagram of the voltage loop.

To get away from the dominant time constants of the DC-link circuit, in accordance with MO criterion, two conditions are imposed in (3):

$$K_p T_i = T_{ed}; \quad T_i T_d = T_{emd} T_{ed} \quad (4)$$

As a result, expression (3) becomes:

$$G_{du}(s) = \frac{K_R \cdot K_{Tu}}{s T_i \cdot (1 + s T_\mu)} \quad (5)$$

On this basis, the transfer function of the closed-loop unity feedback system can be written as:

$$G_u(s) = \frac{1}{1 + 1/G_{du}(s)} = \frac{K_R \cdot K_{Tu}}{K_R \cdot K_{Tu} + s T_i \cdot (1 + s T_\mu)} \quad (6)$$

After expressing the square of the above transfer function modulus,

$$M^2(\omega) = \frac{K_R^2 K_{Tu}^2}{K_R^2 K_{Tu}^2 - \omega^2 T_i (2K_R K_{Tu} T_\mu - T_i) + \omega^4 T_i^2 T_\mu^2} \quad (7)$$

the condition of canceling the denominator term which contain a difference leads to the following expression:

$$T_i = 2K_R K_{Tu} T_\mu \quad (8)$$

Taking also into account the previous conditions given in (4), the other two parameters of the voltage controller are provided, i.e.

$$K_p = \frac{T_{ed}}{T_i} = \frac{T_{ed}}{2K_R K_{Tu} T_\mu}; \quad (9)$$

$$T_d = \frac{T_{ed} T_{emd}}{T_i} = \frac{T_{ed} T_{emd}}{2K_R K_{Tu} T_\mu} \quad (10)$$

B. PI controller design

When a PI controller is chosen, its transfer function is:

$$G_{Ru}(s) = \frac{1 + K_p T_i s}{T_i s} \quad (11)$$

The transfer function of the open-loop unity feedback system takes the following form:

$$G_{du}(s) = \frac{K_R \cdot K_{Tu} \cdot (1 + K_p T_i s)}{(1 + s T_\mu) \cdot s T_i \cdot (1 + T_{ed}s + T_{emd}T_{ed}s^2)} \quad (12)$$

This time, the constant time of the rectifier can be removed by imposing the following condition:

$$K_p T_i = T_\mu. \quad (13)$$

Thus, expression (12) becomes:

$$G_{du}(s) = \frac{K_R K_{Tu}}{s T_i \cdot (1 + T_{ed} s + T_{emd} T_{ed} s^2)}. \quad (14)$$

Then, the transfer function of the closed-loop unity feedback system is expressed as:

$$G_u(s) = \frac{K_R K_{Tu}}{K_R K_{Tu} + s T_i \cdot (1 + T_{ed} s + T_{emd} T_{ed} s^2)}. \quad (15)$$

The square of the transfer function modulus given in (15) can be written as:

$$M^2(\omega) = \frac{K_R^2 K_{Tu}^2}{K_R^2 K_{Tu}^2 - \omega^2 K_2 - \omega^4 K_4 + T_i^2 T_{ed}^2 T_{emd}^2 \omega^6} \quad (16)$$

where:

$$K_2 = T_i \cdot (2K_R K_{Tu} T_{ed} - T_i); \quad (17)$$

$$K_4 = T_i^2 T_{ed} \cdot (2T_{emd} - T_{ed}). \quad (18)$$

It must be noticed that K_4 is positive, as $T_{emd} \gg T_{ed}$.

The condition of removing the coefficient of ω^2 in (16) leads to the following expression of the integral constant:

$$T_i = 2K_R K_{Tu} T_{ed}. \quad (19)$$

After replacing (19) in (13), the expression of the proportional constant is obtained, i.e.:

$$K_p = \frac{T_\mu}{2K_R K_{Tu} T_{ed}}. \quad (20)$$

V. PERFORMANCE OF THE CONTROL SYSTEM

The control system performance, in terms of system response when a prescribed step and ramp voltage is applied, has been tested by using the Simulink model shown in Fig. 3. It is integrated in the global model of the voltage and frequency regulation of the whole induction heating system.

The system parameters are: the line-to-line supply voltage -660 Vrms; the supply frequency - 50 Hz; $R_d = 0.1 \Omega$; $L_d = 0.1$ mH; $C_d = 2000 \mu\text{F}$.

It is important to highlight that the controller's parameters do not depend on the load parameters. Consequently, the tuned voltage controller is unique for all range of pipes to be heated.

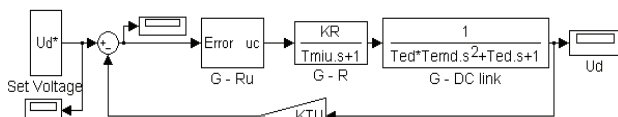


Fig. 3. Simulink model of the voltage control loop.

A. Case of the control system based on PID controller

The PID controller parameters resulted in accordance with expressions (8)-(10) are: $T_i = 2.97$ s; $T_d = 6.73 \cdot 10^{-8}$ s; $K_p = 6.73 \cdot 10^{-5}$.

When a step voltage of 400 V is prescribed, the system response has a half oscillation and shows good performance (Fig. 4).

The overshoot is of about 5% and, after about 16 ms, the inverter input voltage accurately keeps its reference value.

As it can be seen in Fig. 5, the same behavior of the control system is obtained in the case of an increased set voltage of 800 V. Concretely, the overshoot is the same (5%) and the transient duration is increased with about 12.5% (from 16 ms to 18 ms).

The system response was also determined in the case of a voltage ramp input voltage.

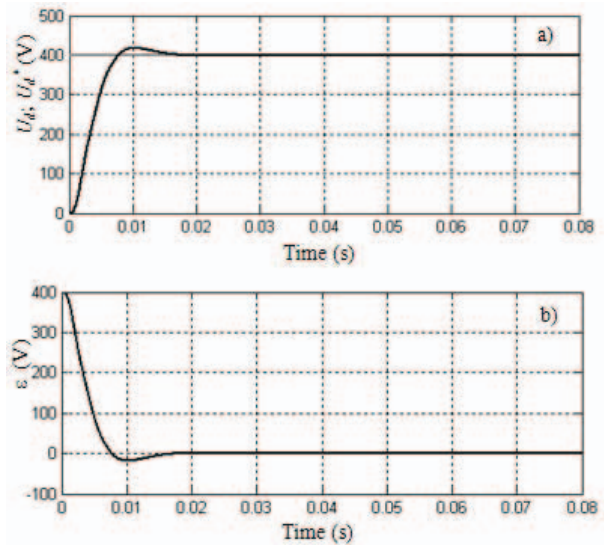


Fig. 4. PID-based control system behavior when a prescribed step voltage of 400 V is imposed: a) Input inverter voltage (in black) and its reference (in gray); b) PID controller input.

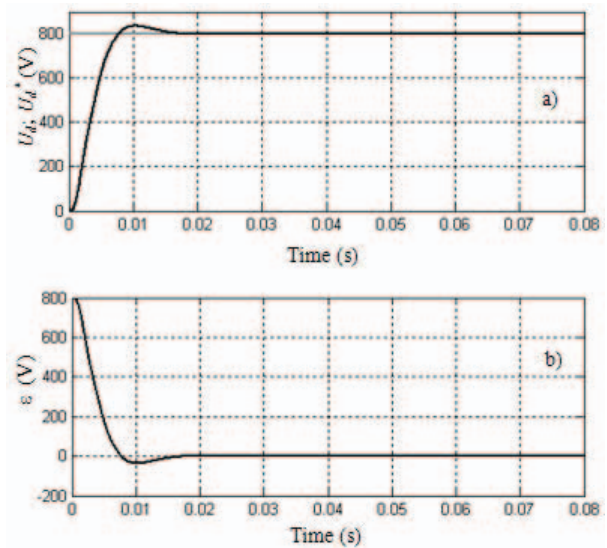


Fig. 5. PID-based control system behavior when a prescribed step voltage of 800 V is imposed: a) Input inverter voltage (in black) and its reference (in gray); b) PID controller input.

The prescribed ramp slope was adopted so that the final value is reached after 0.02 seconds.

As shown in Fig. 6, when the set voltage is 800 V, a low overshoot of about 1.25% occurs and the steady state regime is reached in 0.035 seconds (Fig. 6).

B. Case of the control system based on PI controller

The PI controller parameters resulted in accordance with expressions (19) and (20) are: $T_i = 0.3565$ s; $K_p = 4.67 \cdot 10^{-3}$.

As it can be seen in Fig. 7, the step response of the voltage control system based on a PI controller tuned according to the Modulus Optimum criterion in Kessler variant is totally improper.

The inverter input voltage is unacceptably high and its evolution is oscillatory non-amortized. This is due to the non-elimination of the specific time constant of the DC-link circuit, which resulted in a negative coefficient of the fourth degree term in the numerator of (16).

Starting from the premise that the instability may be due to a too high gain, successive tests have been performed in order to determinate the set of controller parameters that provide an acceptable response for both step and ramp inputs. The results are presented in Fig. 8 – Fig. 11.

As shown in Fig. 8 and Fig. 9, by reducing the proportional time constant and increasing the integral time constant, the system step response becomes stable.

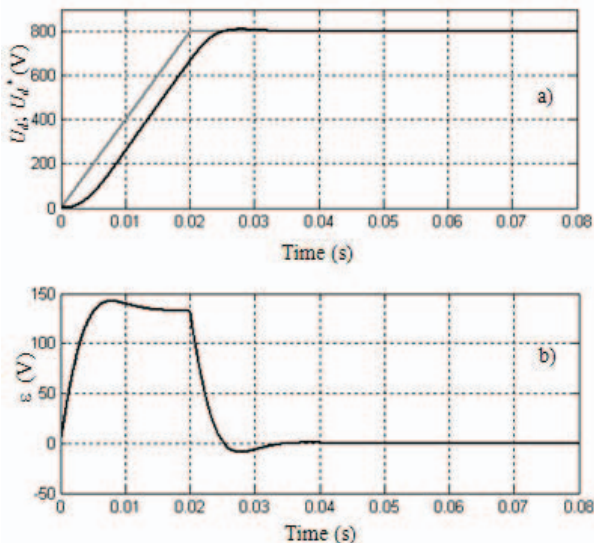


Fig. 6. PID-based control system behavior when a prescribed ramp voltage of 800 V is imposed: a) Input inverter voltage (in black) and its reference (in gray); b) PID controller input.

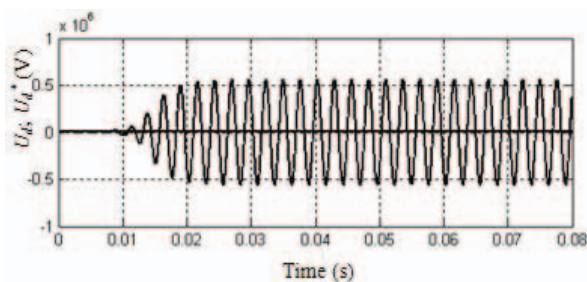


Fig. 7. Response of the PI-based control system when the designed controller parameters are used and a prescribed step voltage of 800 V is imposed.

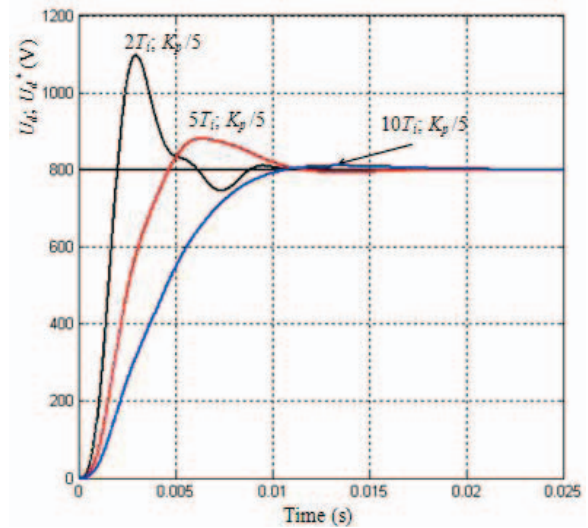


Fig. 8. Response of the PI-based control system when a prescribed step voltage of 800 V is imposed, for $k_p/5$ and three values of T_i .

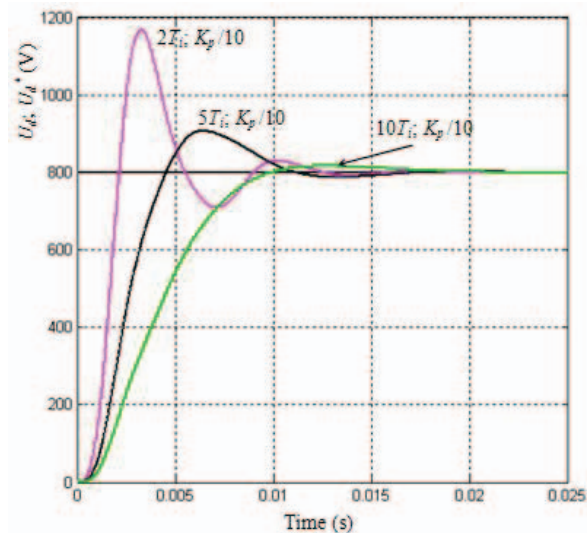


Fig. 9. Response of the PI-based control system when a prescribed step voltage of 800 V is imposed, for $k_p/10$ and three values of T_i .

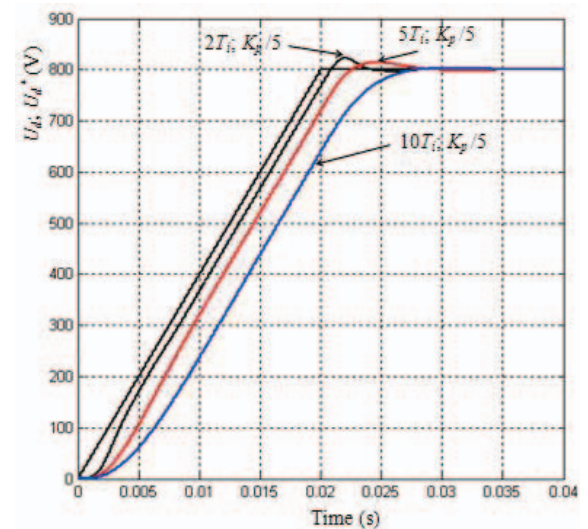


Fig. 10. Response of the PI-based control system when a prescribed ramp voltage of 800 V is imposed, for $k_p/5$ and three values of T_i .

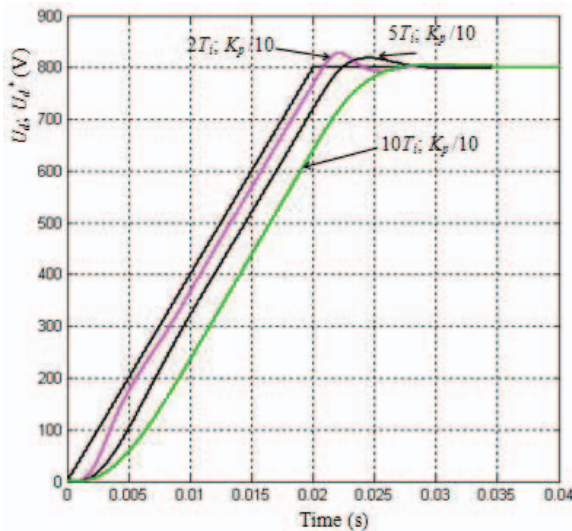


Fig. 11. Response of the PI-based control system when a prescribed ramp voltage of 800 V is imposed, for $k_p/10$ and three values of T_i .

An overshoot below 5% without oscillation is obtained for the pairs $(10T_i, K_p/5)$ and $(10T_i, K_p/10)$. The transient regime duration does not exceed 18 ms.

The controller parameters influence the quality of the ramp response in the same manner (Fig. 10 and Fig. 11).

The best response corresponds to $(10T_i, K_p/5)$, i.e. $T_i = 3.565$ s and $K_p = 0.95 \cdot 10^{-3}$.

VI. CONCLUSIONS

In the induction heating system with square-wave inverter voltage, the control loop of the inverter input voltage directly regulates the rms voltage at inverter output and, consequently, the inverter current and the inductor current.

By adopting a PID voltage controller tuned in accordance with the MO criterion in Kessler variant, the performance of the control system is very good for both step and ramp inputs. When a PI voltage controller is chosen, the controller tuning by successive tests is required and the performances of the control system are worse.

It must be noted that the parameters of the designed voltage controllers do not depend on the inverter load.

As the same inverter input voltage setpoint can be correct for a particular heating pipe and unacceptable to another,

the correspondence between the inverter current and voltage at its input must be known.

REFERENCES

- [1] F.P. Dawson and P. Jain, "A comparison of load commutated inverter systems for induction heating and melting applications," *IEEE Trans. on power electronics*, vol. 6. no. 3, July 1991, pp. 430-441.
- [2] J.M. Espi, E.J. Dede, E. Navarro, E. Sanchis, and A. Ferreres "Features and design of the voltage-fed L-LC resonant inverter for induction heating," *Proc. Power Electronics Specialists Conference*, 1999, pp. 1126 - 1131.
- [3] J.M. Espi, E. Navarro, J. Maicas, J. Ejea, and S. Casans, "Control circuit design of the L-LC resonant inverter for induction heating," *Proc. Power Electronics Specialists Conference*, 2000, pp. 1430-1435.
- [4] J.M. Espi Huerta; E.J. Dede Garcia Santamaria, R. Garcia Gil, and J. Castello Moreno, "Design of the L-LC resonant inverter for induction heating based on its equivalent SRI," *IEEE Trans. on Industrial Electronics*, vol. 54, no.6, 2007, pp. 3178-3187.
- [5] J.M. Espi, E.J. Dede, A. Ferreres, and R. Garcia, "Steady-state frequency analysis of the LLC- resonant inverter for induction heating," *Technical Proc. V IEEE Int. Power Electronics Congress*, 14-17 Oct. 1996, pp. 22-28.
- [6] J. Essadaoui, P. Sicard, E. Ngandui, and A. Cheriti, "Power inverter control for induction heating by pulse density modulation with improved power factor," *IEEE Canadian Conference on Electrical and Computer Engineering*, 4-7 May 2003, vol. 1, pp. 515 - 520.
- [7] S. Peram, V. Ramesh, and J.S. Ranganayakulu, "Full bridge resonant inverter for induction heating applications," *International Journal of Engineering Research and Applications*, vol. 3, issue 1, January-February 2013, pp.66-73.
- [8] Mihaela Popescu, A. Bitoleanu, and M. Dobriceanu, "Analysis and optimal design of matching inductance for induction Heating system with voltage inverter," *The 8th International Symposium on Advanced Topics in Electrical Engineering*, 23-25 May 2013, Bucharest.
- [9] Mihaela Popescu and A. Bitoleanu, "Power control system design in induction heating with resonant voltage inverter," *The 6th International Conference on Advanced Computer Theory and Engineering*, August 2013, Male, to be published.
- [10] A.J.J. Rezek, C.A.D. Coelho, J.M.E. Vicente, J.A. Cortez; And P.R. Laurentino, "The modulus optimum (MO) method applied to voltage regulation systems: modeling, tuning and implementation," *Proc. of Int. Conf. on Power System Transients*, June 2001, pp. 138-142.
- [11] C. Bajracharya, M. Molinas, J.A. Suul, T.M. Undeland, "Understanding of tuning techniques of converter controllers for VSC-HVDC," *Nordic Workshop on Power and Industrial Electronics*, June 9-11, 2008.